

# Orbital Motion in the Radio Galaxy 3C 66B: Evidence for a Supermassive Black Hole Binary

Hiroshi Sudou,<sup>1\*</sup> Satoru Iguchi,<sup>2</sup> Yasuhiro Murata,<sup>3</sup> Yoshiaki Taniguchi,<sup>1</sup>

<sup>1</sup>Astronomical Institute, Graduate School of Science,  
Tohoku University, Sendai 980-8578, Japan

<sup>2</sup>National Astronomical Observatory of Japan,  
Mitaka, Tokyo 181-8588, Japan

<sup>3</sup>Institute of Space and Astronautical Science,  
Sagamihara, Kanagawa 229-8510, Japan

\*To whom correspondence should be addressed; E-mail: sudou@astr.tohoku.ac.jp.

**Supermassive black hole binaries may exist in the centers of active galactic nuclei like quasars and radio galaxies and mergers between galaxies may result in the formation of supermassive binaries during the course of galactic evolution. Using the very-long-baseline interferometer, we imaged the radio galaxy 3C 66B at radio frequencies and found that the unresolved radio core of 3C 66B shows well-defined elliptical motions with a period of  $1.05 \pm 0.03$  years, which provides a direct detection of a supermassive black hole binary.**

The presence of a supermassive black hole binary (or a supermassive binary; SMB) in active galactic nuclei (AGNs) has been suggested mainly by periodic optical and radio outbursts (1,2), wiggled patterns of compact radio jets (i.e., the indication of precession motions of the radio jets) (3,4), and X-shaped morphology of radio lobes (5). AGNs with those characteristics tend to be associated with strong radio jets and thus their host galaxies are often giant elliptical

galaxies (6). If they were made from mergers between or among nucleated galaxies (7,8), they may contain two or more black holes in their central regions because progenitor galaxies may contain a supermassive black hole in their nuclei (9,10). Captured black holes will be settled under dynamical friction in the core of the merged stellar system and then will form a SMB (11). Therefore, it is important to establish the presence of a SMB in an AGN and then investigate the true role of a SMB in AGN activity.

The most direct evidence for a SMB can be obtained by detection of the Kepler orbital motion of some emission component close to black holes. One technical problem is that an expected separation between the two supermassive black holes (e.g.,  $\sim 10^{17}$  cm) is too small to be resolved spatially when we use optical telescope facilities because that separation corresponds to  $\sim 100$  micro-arcsecond ( $\mu\text{as}$ ) if its host galaxy is located at a distance of 100 Mpc (Mpc). However, the use of a technique of phase-referencing very-long-baseline interferometry (VLBI) at radio frequencies allows us to achieve such position measurements with the accuracy of tens of  $\mu\text{as}$  (12). We looked for the Kepler motion of a radio-emission component in a pair of radio sources, 3C 66B and 3C 66A; 3C 66B is a radio galaxy at redshift  $z = 0.0215$  (13), whereas 3C 66A is a more distant BL Lac object at  $z = 0.44$  (14). This pairing allows us to use this source as the stationary position reference to 3C 66B. They are one of best pairs for the phase-referencing VLBI, because they are bright radio sources and their spatial separation is only 6 arc min.

We observed this pair at 2.3 and 8.4 GHz with the very-long-baseline array (VLBA) of the National Radio Astronomy Observatory (NRAO) over six epochs between 13 March 2001 and 14 June 2002. Because the separation between 3C 66A and 3C 66B is smaller than the beam widths of the VLBA antennas at 2.3 and 8.4 GHz (26 and 6 arc min, respectively), it is possible to observe both sources in each antenna beam simultaneously at these frequencies.

The radio core position of 3C 66B at each epoch was measured with respect to that of 3C

66A. We used the local brightest peak in the map, rather than the Gaussian peak, to determine the radio core position. The Gaussian peak may have a larger uncertainty as a result of the effects of asymmetrical structure of the sources.

Time variations of the radio core position in 3C 66B at 2.3 and 8.4 GHz (Fig. 1 and Fig. 2, respectively) can be fitted by an elliptical motion (Table 1). The reduced chi-square value obtained when calculated with the observation error is  $\approx 0.6$  at 2.3 GHz and  $\approx 0.05$  at 8.4 GHz (12). Because these values are less than unity, especially at 8.4 GHz, the position error might have been overestimated. Assuming the reduced chi-square value of unity, we find that the revised position errors,  $\Delta\alpha'$  and  $\Delta\delta'$ , are 71 and 60  $\mu\text{as}$  at 2.3 GHz and 9 and 7  $\mu\text{as}$  at 8.4 GHz, respectively (12). Although the orbital periods at 2.3 and 8.4 GHz are nearly the same, the major axis at 2.3 GHz is about five times as long as that at 8.4 GHz and the position angle of the major axis of the two frequencies differs by  $\approx 24^\circ$ .

The averaged period of the fitted core motion is estimated to be  $1.05 \pm 0.03$  years. Although this period might be interpreted as due to some geodetic effects related to Earth's orbital motion around the sun, such possibilities can be rejected for the following reasons. The annual parallax of 3C 66B cannot explain the observed motion, because the distance of 3C 66B (85 Mpc for the Hubble constant  $H_0 = 75 \text{ km s}^{-1} \text{ Mpc}^{-1}$ ) leads to the amplitude of the annual parallax of only  $\sim 0.01 \mu\text{as}$ . Furthermore, the large difference in the length of the major axis between 2.3 and 8.4 GHz can not be understood from our knowledge of the annual parallax. Only a possible variability of the total electron content (TEC) in the ionosphere may explain this frequency dependence, because the excess path due to the ionosphere is proportional to  $\text{TEC } \nu^{-2}$ , where  $\nu$  is the observing frequency (15). The typical position error due to the ionosphere for the separation of 6 arc min is estimated to be  $0.005 \left(\frac{\nu}{\text{GHz}}\right)^{-2} \mu\text{as}$ , which is negligible (16). Another possibility is that the radio core in 3C 66B is subject to microlensing effects by a star in the Milky Way galaxy near 3C 66B on the celestial plane (17) and is moved by the annual parallax

of the star. We attempted to fit the radio core motion by this microlensing model and obtained the reduced chi-square value of 1.6, corresponding to a chi-square probability of  $\sim 10\%$ . This result indicates that the microlensing model does not explain the sinusoidal core motion as well as it explains the elliptical motion of the radio core.

Because the radio core is located at the root of the jet where the optical depth is unity (18, 19), the radio core at 2.3 GHz is expected to be located at a greater distance from the central engine than that at 8.4 GHz. Thus, a precession motion of the jet provides a natural explanation for the observation that the major axis of the radio core orbit is longer at 2.3 GHz than at 8.4 GHz. Although the orbital major axis should be always perpendicular to the mean jet axis, the observed inclination angle between the mean jet axis and the orbital major axis is estimated to be  $63 \pm 9^\circ$  at 2.3 GHz and  $39 \pm 6^\circ$  at 8.4 GHz (calculated on the basis of a  $50^\circ$  position angle of the jet, which is estimated from the global jet structure at 2.3 GHz). This fact indicates that the observed core motion is not dominated by only the simple precession motion. The most plausible explanation for this result is that the elliptical motion of the radio core is attributable to the combination of the orbital and precession motions of a SMB in 3C 66B, whereas the core motion at 2.3 GHz is dominated by the precession motion of the jet, which at 8.4 GHz is dominated by the orbital motion of the SMB (Fig. 3).

According to Kepler's third law, the observed period can be expressed as,

$$P = 2\pi G^{-1/2} r^{3/2} (M + m)^{-1/2}, \quad (1)$$

where where  $G$  is the gravitation constant,  $r$  is the separation of two orbiting black hole, and  $M$  and  $m$  ( $M \geq m$ ) are the masses of the black holes, respectively. Eq. 1 allows us to determine the mass density  $\rho$  as a function of only  $P$ ,

$$\rho \equiv \frac{M + m}{(4/3)\pi r^3} = \frac{3\pi}{GP^2}. \quad (2)$$

The observed result leads to  $\rho \approx 2 \times 10^{15} M_{\odot} \text{pc}^{-3}$  (where  $M_{\odot}$  is the mass of the Sun), which is larger than those of massive dark objects in NGC 4258 and Sgr A\* (20, 21). Because the radio core motion at 8.4 GHz is believed to reflect the orbital motion of the SMB more than does that at 2.3 GHz, we regard the length of its major axis as the upper limit of the orbital radius of the SMB. Assuming that the less massive black hole emanates the jet, we obtain the upper limit of the separation and the mass of the SMB of  $r_{\text{max}} \approx 5.4(1 + q) \times 10^{16}$  cm and  $M_{\text{max}} \approx 4.4(1 + q)^2 \times 10^{10} M_{\odot}$ , respectively, where  $q \equiv \frac{m}{M}$  is the mass ratio between the objects. We note that these parameters are similar to those of a radio-loud AGN, OJ 287, which is believed to be an archetypical AGN with a SMB (22). This conclusion is consistent with 3C 66B's being a giant elliptical galaxy which suggests a galaxy merger.

The SMB in 3C 66B will merge into one as a result of the gravitational radiation loss. The lifetime in this evolution phase can be estimated by the relation in Eq. 3 (23).

$$t_{\text{GR}} \approx 7.2 \times 10^4 \left( \frac{M}{10^8 M_{\odot}} \right)^{-3} \left( \frac{r}{10^{16} \text{ cm}} \right)^4 \frac{1}{q(1 + q)} \text{ yr}. \quad (3)$$

If we adopt  $q = 0.1$ , we obtain  $r_{\text{max}} = 5.9 \times 10^{16}$  cm and  $M_{\text{max}} = 5.4 \times 10^{10} M_{\odot}$ . These values give us  $t_{\text{GR}} \simeq 5$  yr for the SMB in 3C 66B. This time scale seems to be extremely short compared with a whole life time of a SMB system (13). A more reasonable lifetime would be obtained for smaller values of  $q$  and/or  $r$ . Combining Eq. 1 and Eq. 3, we find  $t_{\text{GR}} \propto r^{-5}$ . If the true  $r$  is a quarter of the corresponding value for the upper limit, a lifetime  $\sim 10^3$  times as long is obtained. The expected maximum amplitude of gravitational radiation from 3C 66B will be  $\langle h \rangle \sim 10^{-11}$  just before the two black holes merge into one (24, 25).

## References and Notes

1. A. Sillanpää, S. Haarala, M. J. Valtonen, B. Sundelius, G. G. Byrd, *Astrophys. J.* **325**, 628 (1988).

2. E. Valtaoja, *et al.*, *Astrophys. J.* **531**, 744 (2000).
3. N. Roos, J. S. Kaastra, C. A. Hummel, *Astrophys. J.* **409**, 130 (1993).
4. Z. Abraham, *Astron. Astrophys.* **355**, 915 (2000).
5. D. Merritt, R. D. Ekers, *Science* **297**, 1310 (2002).
6. C. M. Gaskell, in *Jets from Stars and Galactic Nuclei*, W. Kundt, Ed. (Springer-Verlag, New York, 2002), p 165
7. D. B. Sanders, *et al.*, *Astrophys. J.* **325**, 74 (1988).
8. Y. Taniguchi, S. Ikeuchi, Y. Shioya, *Astrophys. J.* **514**, L9 (1999).
9. J. Kormendy, D. Richstone, *Annu. Rev. Astron. Astrophys.* **33**, 581 (1995).
10. M. J. Rees, *Annu. Rev. Astron. Astrophys.* **22**, 471 (1984).
11. M. C. Begelman, R. D. Blandford, M. J. Rees, *Nature* **287**, 307 (1980).
12. Materials and Methods are available as supporting material in *Science Online*.
13. T. A. Matthews, W. W. Morgan, M. Schmidt, *Astrophys. J.* **140**, 35 (1964).
14. H. R. Miller, B. Q. McGimsey, *Astrophys. J.* **220**, 19 (1978).
15. A. R. Thompson, J. M. Moran, G. W. Swenson, in *Interferometry and Synthesis in Radio Astronomy*, (Wiley, New York, 1986) p 554
16. The excess path in the zenith direction due to ionosphere is  $l(\nu) = 40.3 \text{ TEC } \nu^{-2}$  (15). As a result of the Doppler shift by the Earth's spin, a frequency shift between two sources occurs, given by  $\nu' = \nu(1 + \omega\theta D/c)$ , where  $D$  is the baseline length, and  $\omega$  is the angular velocity of the Earth spin. Thus, dividing  $l(\nu) - l(\nu')$  by  $c$ , we obtain the time delay due to ionospheric excess path. We assumed that TEC in the zenith direction is  $6 \times 10^{17} \text{ m}^{-2}$ .

17. S. Refsdal, *Mon. Not. R. Astron. Soc.* **128**, 295 (1964).
18. A. Königl, *Astrophys. J.* **243**, 700 (1981).
19. A. P. Lobanov, *Astron. Astrophys.* **330**, 79 (1998).
20. M. Miyoshi, *et al.*, *Nature* **373**, 127 (1995).
21. A. M. Ghez, M. Morris, E. E. Becklin, A. Tanner, T. Kremenek, *Nature* **407**, 349 (2000).
22. H. J. Lehto, M. J. Valtonen, *Astrophys. J.* **460**, 207 (1996)
23. 23. Q. Yu, *Mon. Not. R. Astron. Soc.* **331**, 935 (2002).
24. K. P. Thorne, V. B. Braginsky, *Astrophys. J.* **204**, L1 (1976).
25. T. Fukushige, T. Ebisuzaki, *Astrophys. J.* **396**, L61 (1992)
26. Supported by a grant-in-aid for Fellows of the Japan Society for the Promotion of Science from the Japanese Ministry of Education, Culture, Sports, and Science. NRAO is a facility of the National Science Foundation, operated under cooperative agreement by Associated Universities, Inc. We acknowledge anonymous reviewers for useful suggestions.

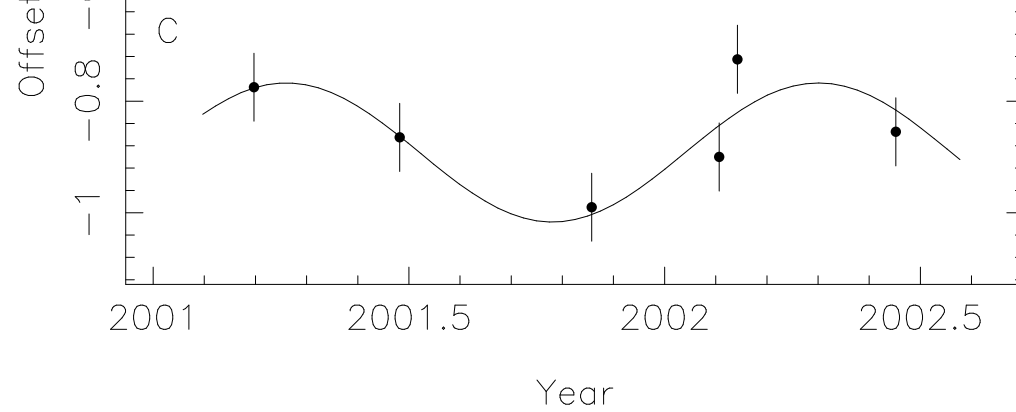
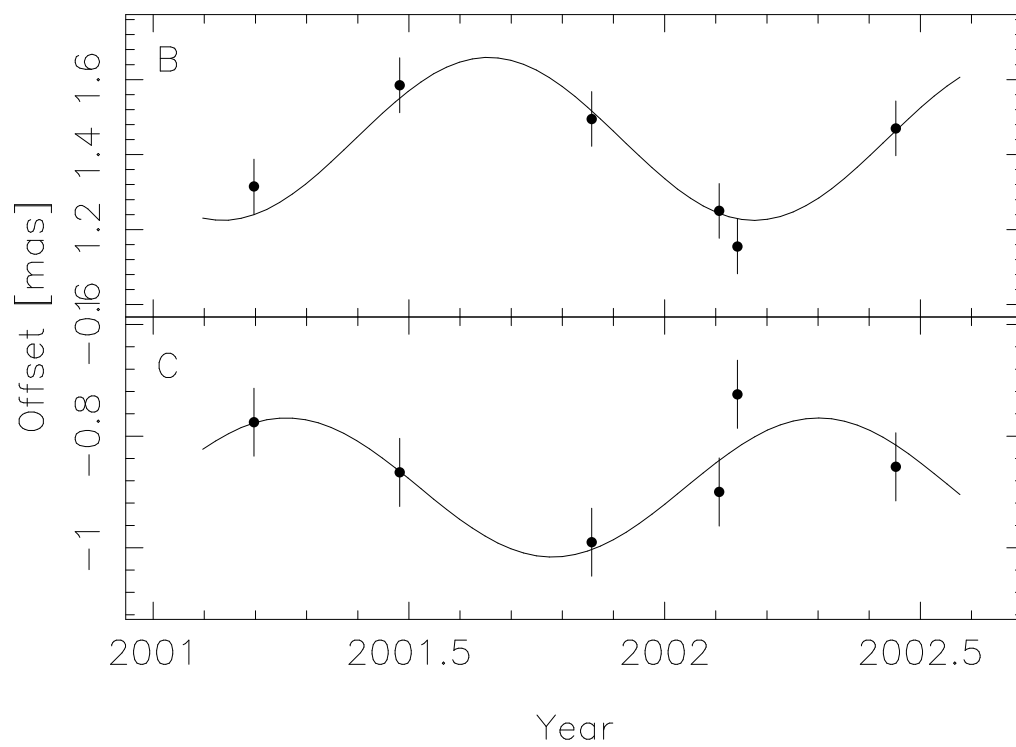
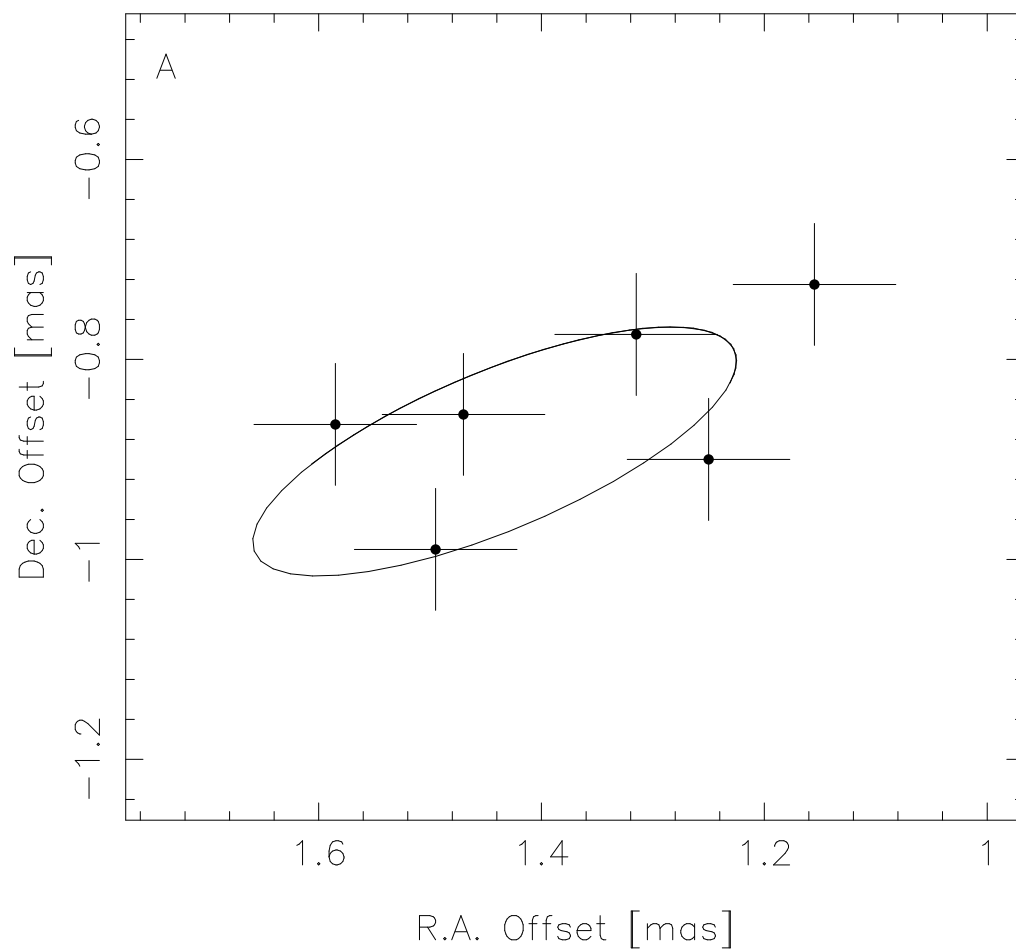
Table 1: Parameters of the fitted orbital motion of the radio core in 3C 66B. The errors in the parameters correspond to a change of 1 in chi-square from the value at the best fitted parameter. The offset angle is the angle between the major axis and the point where the orbital motion started. R.A. center is the relative position in right ascension. Dec. center is the relative position in declination.

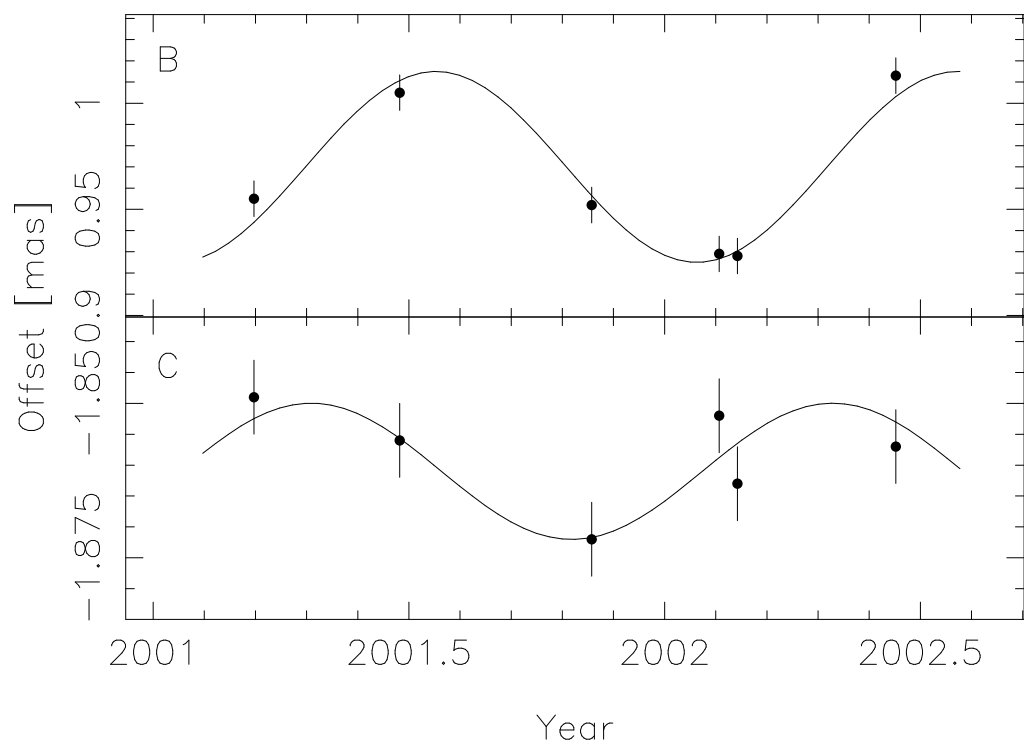
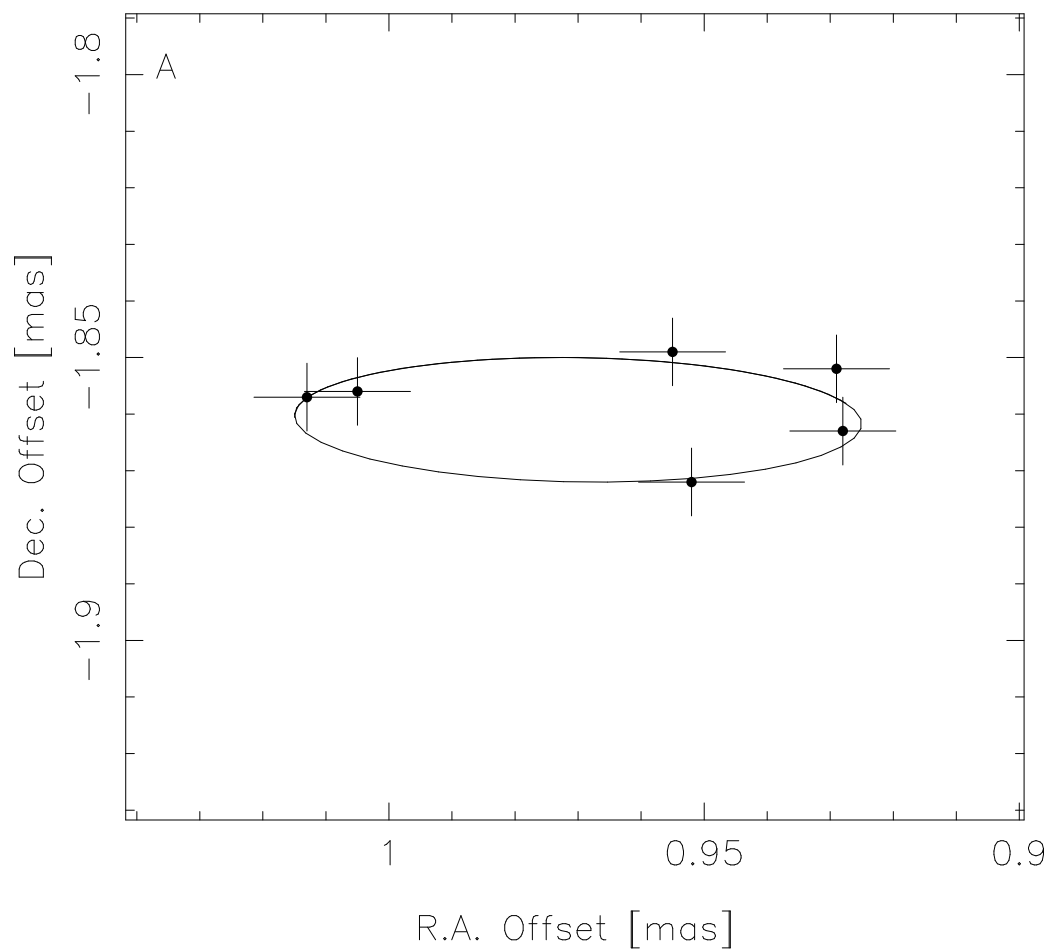
		2.3 GHz	8.4 GHz
Major axis	( $\mu\text{as}$ )	$243\pm 30$	$45\pm 4$
Axial ratio		$0.31\pm 0.17$	$0.24\pm 0.14$
Orbital period	(yr)	$1.10\pm 0.06$	$1.02\pm 0.04$
Position angle	( $^\circ$ )	$113\pm 9$	$89\pm 6$
Offset Angle	( $^\circ$ )	$60\pm 7$	$101\pm 5$
R.A. center	(mas)	$1.441\pm 0.020$	$0.970\pm 0.002$
Dec. center	(mas)	$-0.888\pm 0.033$	$-1.861\pm 0.004$

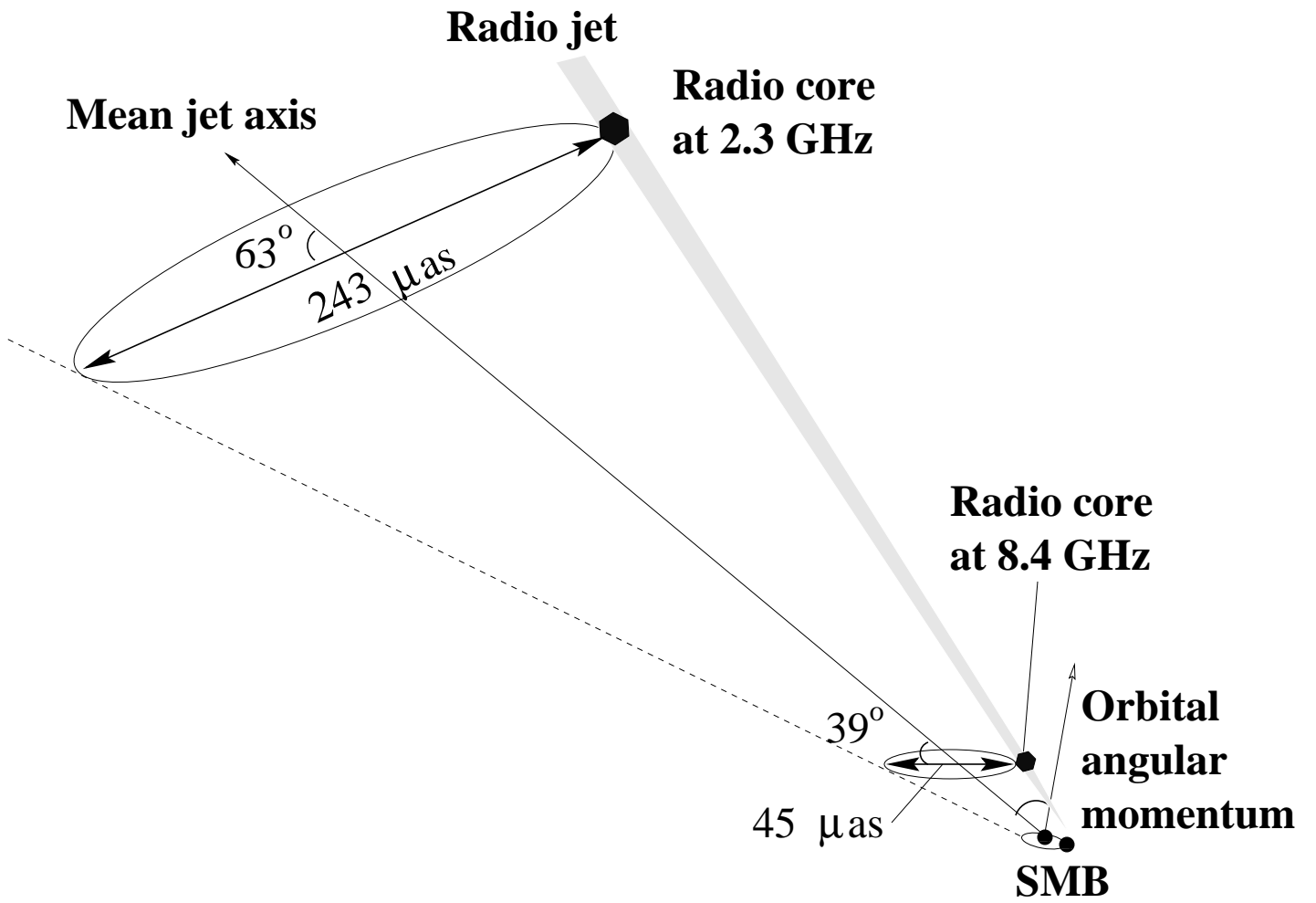
**Fig. 1.** Orbital fit calculations applied to the data of the position change of the core at 2.3 GHz. Observations were carried out on 13 March, 25 June, and 9 November 2001, and 8 February, 21 February, and 14 June 2002. We show (A) spatial distribution, (B) time evolution toward right ascension direction, and (C) time evolution toward declination direction. The error bars indicate the revised position errors suggested from the chi-square value; 71 and 60  $\mu\text{as}$  at 2.3 GHz and 9 and 7  $\mu\text{as}$  at 8.4 GHz, in right ascension and declination, respectively (12).

**Fig. 2** Same as Fig. 1, but at 8.4 GHz.

**Fig. 3** A schematic view of the geometrical relation between the radio core motion and the SMB. Because the orbital velocity of the SMB is added to the intrinsic jet velocity, the jet precession can be induced with the same period as that of the SMB orbital motion (3). Therefore, if the radio core is far enough from the SMB, the orbital major axis of the radio core should be observed as perpendicular to the mean jet axis, as is the normal precession. However, if the radio core is very close to the SMB, it should be observed as almost parallel to the orbital plane of the SMB. Therefore, the position angle of the radio core orbit depends on the distance between the radio core and the SMB, if the jet direction misaligns with the angular momentum vector of the SMB orbit.







## Materials and Methods

### *Phase-referencing VLBI*

In conventional observations with VLBI, the correlated phase is affected by fluctuations due to water vapor in the troposphere and the fluctuations strongly limit the quality and the dynamic range of images. The most effective method to eliminate the tropospheric fluctuations can be made by observing simultaneously a target source and another radio source (e.g., a different quasar) which is close to the target on the celestial plane. This procedure is called as the phase-referencing technique in VLBI observations ( $S1, S2$ ). In principal, assuming that the atmospheric phase fluctuation is almost the same between the two sources, we eliminate it by subtracting the phase of the target from that of the near radio source.

In our observations, the data of 3C 66A were first reduced by using the standard hybrid mapping method and self-calibration procedures with the minimum integration time of 6 seconds available on the NRAO AIPS. We thus obtained antenna-based solutions including the atmospheric phase fluctuation. Then these solutions were directly applied to the observations of 3C 66B and the final phase-referencing map of 3C 66B was obtained (Fig. S1).

### *Error analysis*

The dominant uncertainty of the position measurement in the phase-referencing observation comes from unmodeled source structure in the map. In order to examine this uncertainty, we compare the local brightest peak with the centroid of the strong CLEAN components (more than 25 % of the maximum one) ( $S3, S4$ ). This procedure gives nominally us the observational position errors,  $\Delta\alpha$  in right ascension and  $\Delta\delta$  in declination, 91  $\mu\text{as}$  and 76  $\mu\text{as}$  at 2.3 GHz and 40  $\mu\text{as}$  and 28  $\mu\text{as}$  at 8.4 GHz, respectively.

On the other hand, we derived the standard phase errors from theoretical estimates based on models of the propagation medium and the geometry of the array, e.g., tropospheric and ionospheric effects, uncertainties of antenna positions, the time difference between atomic time and universal time, and the polar motion or the nutation of the Earth. The misidentification of the reference point in maps due to finite signal-to-noise ratio also contributes to the position error. Assuming the typical weather and geodetic conditions in VLBA observations, we calculate the corresponding position error in the simultaneous observations of the source pair with the separation of 6 arcminute.

The standard position errors,  $\Delta\alpha$  in right ascension and  $\Delta\delta$  in declination, are estimated to be  $10 \mu\text{as}$  and  $16 \mu\text{as}$  at 2.3 GHz and  $7 \mu\text{as}$  and  $12 \mu\text{as}$  at 8.4 GHz, respectively.

As shown in the text, assuming that the reduced  $\chi^2$  value for the core motion fitting is unity, we find that the revised position errors,  $\Delta\alpha'$  and  $\Delta\delta'$ , are  $71 \mu\text{as}$  and  $60 \mu\text{as}$  at 2.3 GHz and  $9 \mu\text{as}$  and  $7 \mu\text{as}$  at 8.4 GHz, respectively. The revised errors at 8.4 GHz is comparable to the theoretical standard errors, suggesting that the uncertainty due to complex source structure is excluded in the data at 8.4 GHz. In contrast, the position measurement at 2.3 GHz seems to contain effect of unresolved jet structure in the radio core component.

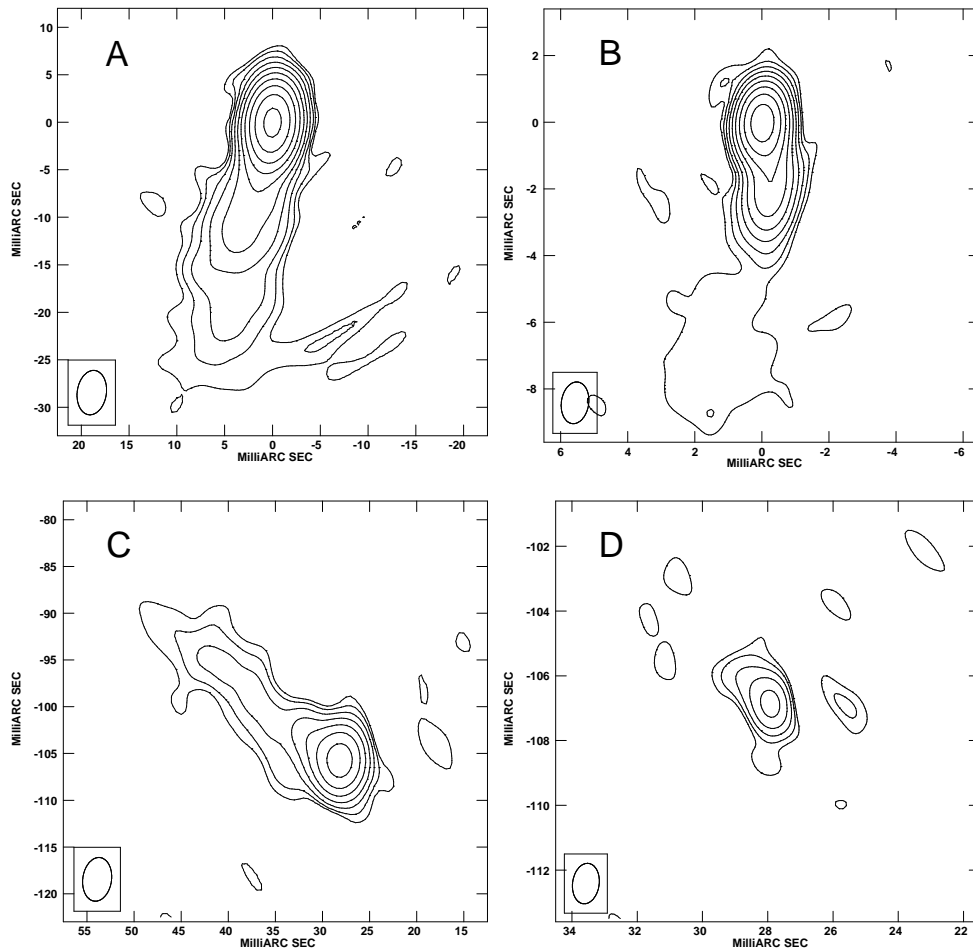


**Fig. S1** Phase-referencing images of 3C 66A at (A) 2.3 GHz and (B) 8.4 GHz and 3C 66B at (C) 2.3 GHz and (D) 8.4 GHz, obtained at the 5th epoch (21 February 2001). The contours are  $(1, 2, 4, 8, 16, 32, 64, 128, 256, 512) \times 3\sigma$  errors. The synthesized beam is plotted at the bottom left of each image, with an approximately  $5.4 \times 3.3 \text{ mas}$ , P.A. =  $-8^\circ$  at 2.3 GHz and  $1.3 \times 0.8 \text{ mas}$ , P.A. =  $-8^\circ$  at 8.4 GHz.

## References

- S1. W. Alef, in NATO ASI Ser., Very Long Baseline Interferometry, Techniques and Applications, eds. M. Felli & R. E. Spencer (The Netherlands: Kluwer Academic Publishers, 1989), p 261
- S2. A. J. Beasley, & J. E. Conway, in ASP Conf. Ser. 82, Very Long Baseline Interferometry and the VLBA, eds. J. A. Zensus, P. J. Diamond, & P. J. Napier (San Francisco, 1995), p 328
- S3. J. C. Guirado, *et al.*, *Astron. Astrophys.* **293**, 613 (1995).
- S4. M. J. Rioja, R. W. Porcas, *Astron. Astrophys.* **355**, 552 (2000).